Front. Chem. Sci. Eng. 2017, 11(4): 633–646
https://doi.org/10.1007/s11705-017-1620-8

REVIEW ARTICLE

Functional ferritin nanoparticles for biomedical applications

Zhantong Wang[1,2], Haiyan Gao[1], Yang Zhang[1], Gang Liu (✉)[1], Gang Niu[2], Xiaoyuan Chen (✉)[2]

1 State Key Laboratory of Molecular Vaccinology and Molecular Diagnostics & Center for Molecular Imaging and Translational Medicine, School of Public Health, Xiamen University, Xiamen 361102, China
2 Laboratory of Molecular Imaging and Nanomedicine (LOMIN), National Institute of Biomedical Imaging and Bioengineering (NIBIB), National Institutes of Health, Bethesda, MD 20892, USA

Abstract Ferritin, a major iron storage protein with a hollow interior cavity, has been reported recently to play many important roles in biomedical and bioengineering applications. Owing to the unique architecture and surface properties, ferritin nanoparticles offer favorable characteristics and can be either genetically or chemically modified to impart functionalities to their surfaces, and therapeutics or probes can be encapsulated in their interiors by controlled and reversible assembly/disassembly. There has been an outburst of interest regarding the employment of functional ferritin nanoparticles in nanomedicine. This review will highlight the recent advances in ferritin nanoparticles for drug delivery, bioassay, and molecular imaging with a particular focus on their biomedical applications.

Keywords nanomedicine, ferritin, drug delivery, bioassay, molecular imaging

1 Introduction

Ferritin, the primary iron storage protein, first discovered by Laufberger in 1937 [1], was isolated from horse spleen. Ferritins can be found throughout the animal, plant, and microbial kingdoms. The iron storage protein ferritin consists of a spherical polypeptide shell (Apoferritin) surrounding a 6-nanometer inorganic core of the hydrated iron oxide ferrihydrite ($5Fe_2O_3 \cdot 9H_2O$) [2,3]. There are two types of ferritins in mammalian cells, H and L, these two ferritins have complementary functions in iron uptake process. The H chain contains a dinuclear ferroxidase site that is located within the four-helix bundle of the subunit; it catalyzes the oxidation of ferrous iron by O_2, producing H_2O_2. The L subunit lacks this site but contains additional glutamate residues on the interior surface of the protein shell which produce a microenvironment that facilitates mineralization and the turnover of iron (III) at the H subunit ferroxidase site [4]. Consequently, the L chain ferritin has less iron than the H ferritin.

Different ferritins from different species possess varieties in amino acid sequences but similarity in architectures. Members of the ferritin superfamily are spherical proteins composed of 24 subunits of mass 450–500 kDa with an outer diameter of about 12 nm and interior cavity diameter of about 8 nm (Fig. 1) [5]. The protein shell can possess up to 4500 iron atoms within its 8-nm-diameter cavity, while this capacity is not always utilized to the full, ferritin preparations usually take less than 3000 iron atoms [6]. Iron gains entry to the interior of ferritins through the eight hydrophilic channels that traverse the protein shell. The unique architecture of ferritin provides two interfaces, one outside and one inside, for possible functional loading. The outer surface of ferritin can be chemically or genetically modified with functional motifs, and the cavity of the ferritin can be loaded with a wide range of metals and small molecules with high affinity [7–14].

Besides the characteristic architecture, ferritins possess

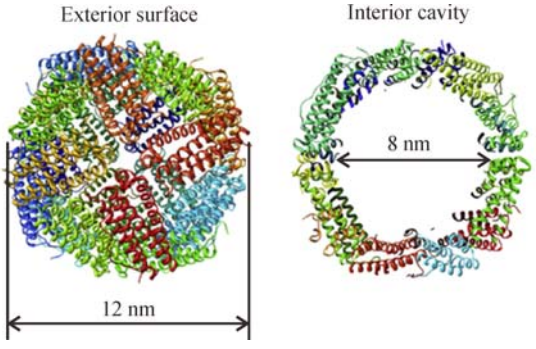

Fig. 1 Scheme structure of human H chain ferritin. Adapted from ref. [5] with permission

Received September 27, 2016; accepted November 13, 2016

E-mails: gangliu.cmitm@xmu.edu.cn (Liu G), shawn.chen@nih.gov (Chen X)

unique properties physically and chemically. Unlike most other proteins, which are sensitive to harsh temperature and pH, ferritins are able to bear high temperatures up to 75 ºC for 10 min and is stable in various denaturants such as urea, sodium hydroxide, and guanidinium chloride. These unique features are owing to the fact that ferritin contains large numbers of salt bridges and hydrogen bonds formed between subunits [15]. One of the most amazing features of ferritin is that the protein architecture can be broken down in an acidic environment (around pH 2.5) and restored, almost completely, by returning the pH back to physiological conditions (around pH = 7.5) [16]. These unique properties enquire ferritin an ideal and mighty nanoplatform in many fields, including constrained synthesis, nanodevices, disease diagnosis and therapy, drug delivery, vaccine development, bioassay, etc.

The ferritin nanoparticles used in constrained synthesis, nanodevices [5,17–21], have been summarized in several excellent review articles and will not be discussed here. In this article, we will focus on the use of ferritin nanoparticles in the fields of drug delivery, vaccine development, bioassay, disease diagnosis and therapy with molecular imaging methods (Fig. 2).

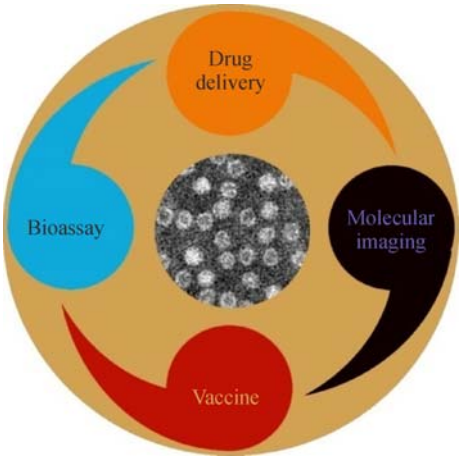

Fig. 2 Schematic representation of nanomedicine applications of functional ferritin nanoparticles

2 Ferritin nanoparticles used in drug delivery

Ferritin, with an internal diameter of 8 nm, when expressed artificially in iron-free conditions, the yielded apoferritins are hollow, comprising a cavity that can be loaded with different species. Furthermore, ferritin-binding sites and the endocytosis of ferritin have been identified in tumor cells [22–25]. The association between ferritin and membrane-specific receptors lead the ferritin internalization to some tumor tissues [26]. Consequently, apoferritin could be a promising vehicle for targeted drug delivery, moreover, the outer surface of ferritin can be chemically or genetically modified with targeting motifs, makes the targeting process more precise.

Integrins $\alpha_v\beta_3$ and $\alpha_v\beta_5$ are up-regulated in angiogenic tumor vasculature [27,28]. RGD-4C peptide (CDCRGDCFC) [7] that selectively binds to integrins $\alpha_v\beta_3$ and $\alpha_v\beta_5$ was incorporated into the *N*-terminus of the human ferritin subunit. As the *N*-terminus of the human ferritin is exposed to the exterior surface of the assembled ferritin cage, each ferritin cage would have 24 copies of RGD-4C peptides for multivalent integrin interactions. With the targeting peptide on ferritin, the ferritin nanoparticles showed much stronger binding affinity to tumor cells than normal cells. This suggests that the exterior surfaces of protein cage architectures can be modified without altering the structure, and furthermore, with its unique property that the protein architecture can be broken down in an acidic environment and restored by returning the pH back to neutral environment, which showed that it is possible to add multifunctionality such as cell targeting, imaging, and perhaps therapeutic agents simultaneously to a single protein cage [29].

Zhen et al. [12] used ferritin as a drug delivery vehicle to encapsulate doxorubicin (Dox). Dox is a wide-spectrum anticancer antibiotic. Dox molecules were efficiently loaded into ferritin nanocages with Cu (II) as a helper agent. The integrin targeting peptide RGD4C and near-infrared (NIR) dye ZW800 (ex/em: 780/800 nm) [30] were also conjugated to the exterior of ferritin (Fig. 3(a)). With the incorporation of Dox and NIR dye and the modification of RGD targeting motif, ferritin behaved as a functional tumor theranostic agent (Fig. 3(b)).

Besides this Dox encapsulated ferritin, other drugs such as photosensitizers can also be loaded to ferritins. Photodynamic therapy (PDT) contains three components, a photosensitizer (PS), light, and oxygen. With a laser light of a particular wavelength irradiated on the PS, PSs are activated, producing reactive oxygen species (ROS) such as $^1O_2$, which are cytotoxic and capable of killing nearby cells [31]. PDT has been used in the treatment of many types of diseases including cancer [32–34]. Zhen et al. [13] used ferritin to encapsulate and deliver PSs. With this method, PDT against cancer was achieved. They used RGD4C modified ferritin to encapsulate zinc hexadecafluoro-phthalocyanine ($ZnF_{16}Pc$). $ZnF_{16}Pc$ is a hydrophobic PS, but with 60 wt-% loading rate in ferritin. With RGD4C motif on the surface of ferritin, $ZnF_{16}Pc$ loaded RGD4C-ferritin showed remarkable tumor accumulation rate as well as good tumor inhibition rate. On the other hand, $ZnF_{16}Pc$ loaded RGD4C-ferritin also showed negligible toxicity to the skin and other major organs. With the successful loading of Zn based metal-containing PS into ferritin, it is possible for ferritin to load many different metal-containing PSs with the help of metal binding sites in them.

Besides RGD peptide, other targeting ligands can also be used to modify ferritin for tumor specific delivery of

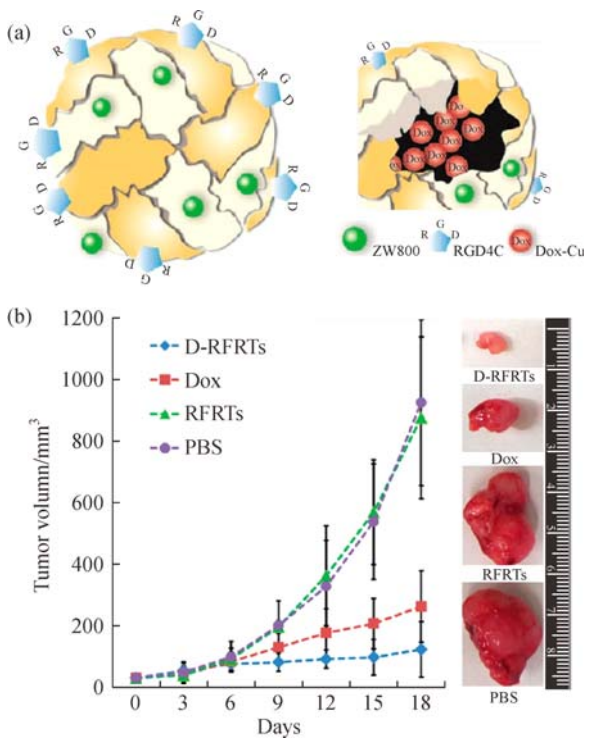

Fig. 3 (a) Schematic illustration of Cu-DOX loaded, RGD and ZW800 modified ferritin (FRT) nanoparticle; (b) therapeutic studies on U87MG tumor-bearing mice. Significant difference in tumor growth was found between Dox-loaded RFRTs (D-RFRTs) treated mice and those treated with PBS, RGD4C modified FRTs (RFRTs) and free Dox ($P < 0.05$) on day 18. Adapted from ref. [12] with permission

drug molecules. For example, Falvo et al. [35] developed an antibody linked ferritin to encapsulate cisplatin to target melanoma, which is the primary cause of death in patients with skin cancer [36].

Malignant melanoma is rising at a high speed much faster than any other cancers in the US, and it becomes a severe public health problem [37,38]. With the rising tendency, about 1.4% people will get melanoma in his or her life [39]. Chondroitin sulphate proteoglycan 4 (CSPG4) is a transmembrane cell surface proteoglycan with a glycoprotein core [40], and it regulates cell spreading through many signaling pathways [41,42]. Melanoma cells are often $CSPG4^+$ [43], and antibodies against CSPG4 have been well developed [44,45]. On the other hand, cisplatin is one of the most effective cytotoxic agents against many cancers, but its chemical instability, poor water solubility and low lipophilicity restrict its clinical applications. After coupling CSPG4 monoclonal antibody (mAb) to human ferritin, and with the inner cavity encapsulated with cisplatin molecules, this antibody-ferritin-cisplatin conjugate showed specific binding to a $CSPG4^+$ melanoma cells and remarkably inhibited the growth of $CSPG4^+$ tumors. The same formula was only modestly effective in treating $CSPG4^-$ tumors, which is likely due to the enhanced permeability and retention (EPR) effect of ferritin nanoparticle formula [46].

Various drug loading studies suggest that ferritin is a safe and effective carrier. With the ease of modification, different targeting moieties can be conjugated on the exterior surface of ferritin. Also the multi binding sites of ferritin allow loading a variety of therapeutics to improve the treatment of diseases. More importantly, ferritin has negligible toxicity and immunogenicity profiles, which enable it much fewer concerns than usual drug carriers in clinical translation.

3 Ferritin nanoparticles used in vaccine development

Nanotechnology increasingly plays a significant role in vaccine development in the past decade, leading to the birth of "nanovaccinology" [47]. The use of nanoparticles in vaccine formulations is expected to have improved antigen stability and immunogenicity, targeted delivery and slow release property [48–50]. There have been many types of nanoparticle used in the field of vaccine development [51], including polymeric nanoparticles [52–54], inorganic nanoparticles [55,56], liposomes [57], virus-like particles [58,59], self-assembled proteins [60], etc. Ferritin, with its particle uniformity and inner/outer surface modifiable features, can play an important role in the field of vaccine development.

Kanekiyo et al. [61] used *Helicobacter pylori* non-haem ferritin [62] to develop a vaccine which can elicit broadly neutralizing H1N1 antibodies. Haemagglutinin of influenza virus was inserted at the interface of adjacent subunits so that eight trimeric viral spikes are formed on the surface of ferritin nanoparticle during the spontaneous assembly process. Immunization with this influenza-ferritin nanoparticle vaccine produced haemagglutination inhibition antibody titers of one magnitude higher than those from the licensed inactivated vaccine.

Dendritic cells (DCs) are the most potent professional antigen-presenting cells that initiate and control antigen-specific immune responses. DCs plays an important role in internalizing, processing, and presenting antigens to naive T cells and inducing their proliferation and differentiation into effector cells, such as $CD8^+$ cytotoxic T cells to kill infected target cells or $CD4^+$ helper T cells to secrete cytokines and facilitate diverse forms of cellular and humoral immunity [63]. DC-based vaccine development has been a promising approach to direct antigen-specific adaptive immunity *in vivo* [64,65]. Han et al. [66] used ferritin nanoparticles to display different ovalbumin antigens. The ovalbumin antigenic peptides OT-1 ($Ovalbumin_{257\text{-}264}$) [67] and OT-2 ($Ovalbumin_{323\text{-}339}$) [67] were genetically introduced either onto the exterior surface or into the interior cavity of ferritin, and the nanoparticles were effectively delivered to DCs and processed within

endosomes, followed by successful induction of antigen-specific $CD8^+$ or $CD4^+$ T cells. On the other hand, this ferritin-OT nanoparticle immune effect was also confirmed on mice. Immunized with ferritin-OT1 peptides efficiently differentiated OT-1 specific $CD8^+$ T cells into functional effector cytotoxic T cells, resulting in selective killing of antigen-specific target cells. Immunized with ferritin-OT2 peptides resulted in the differentiation of proliferated OT-2 specific $CD4^+$ T cells into functional $CD4^+$ Th1 and Th2 cells which was confirmed by the detection of the cell-produced IFN-γ/IL-2 and IL-10/IL-13 cytokines.

4 Ferritin nanoparticles used in bioassay

Enzyme-linked immunosorbent assay (ELISA) is currently one of the most popular methods for biomarker detection; however, it has relatively poor sensitivity. Many new bioassay methods with improved sensitivity have recently emerged [13,68]. Ferritin nanoparticles with unique physiochemical properties can be used in ultrasensitive biomarker detection [69–72].

Liu et al. [73] developed a sensitive protein detection method based on marker-loaded apoferritin nanoparticles. Briefly, ferritin nanoparticles were first loaded with a fluorescence marker (fluorescein anion) and a redox marker [hexacyanoferrate (III)], and then labeled with NHS-biotin. When used in biomarker detection, primary antibody was coated on the glass or on the magnetic beads. After adding the antigen and biotinylated secondary antibody, streptavidin was applied as a bridge to bind two or three biotin-functionalized apoferritin nanoparticles. With different markers loaded in the apoferritin, the antigen of interest can be detected by fluorescence immunoassay and electrochemical immunoassay, both of which have comparable sensitivities. Similarly, Liu et al. [74] also developed a metal (cadmium and lead) phosphate loaded apoferritin for highly sensitive electrochemical immunoassay detection of protein biomarkers (Fig. 4). With the precise control of the synthesis, bioinorganic nanocomposites were obtained, and labeled with biotin, with the similar detection method described above, tumor necrosis factor (TNF-α) as the protein marker was detected. TNF-α is believed to have an important role in the pathogenesis of severe infectious disease [75]. With this electrochemical immunoassay, the detection limit of TNF-α is around 2 pg/mL, which is about twenty times lower than the standard ELISA kit [76].

Besides the protein markers, sequence-specific DNA can also be detected with the help of ferritin nanoparticles. Yu et al. [77] developed a DNA detection method based on gold nanoparticles and cadmium loaded apoferritin. Briefly, the target DNA was sandwiched between capture DNA coupled to magnetic beads and signal DNA self-assembled on gold nanoparticles, and the gold nanoparticles were incorporated with marker-loaded apoferritin

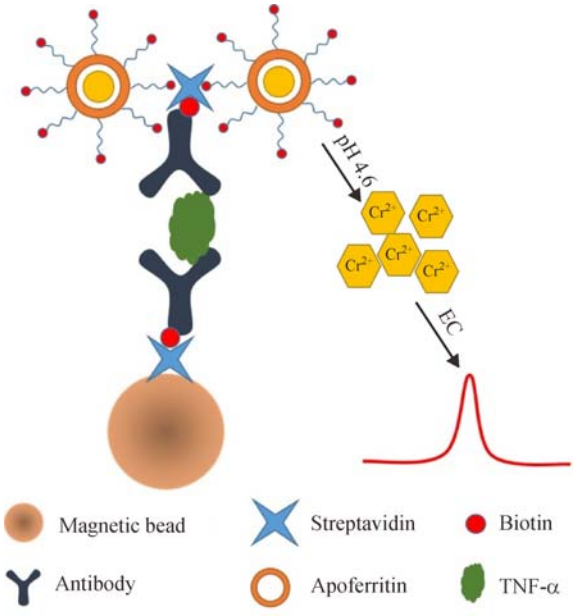

Fig. 4 Schematic illustration of the electrochemical immunoassay protocol. The avidin-modified magnetic beads are linked to biotinylated TNF-α primary antibody. The biotinylated secondary TNF-α antibody is coupled to cadmium phosphate–apoferritin nanoparticle labels using streptavidin as a bridge. The sandwich complex containing TNF-α antigen is then separated by magnetic field followed by electrochemical measurement at pH 4.6, at which cadmium ions are released in situ and detected by a plated mercury film electrode. Adapted from ref. [74] with permission

nanoparticles. After the hybridization, the nanostructure was dispersed in acetate buffer (pH = 4.6), and the cadmium was released from the apoferritin, with the presence of $HgCl_2$, the Cd^{2+} can be detected which reflects the DNA level. Under the optimum conditions, the DNA biosensor has a linear range from 2.0×10^{-16} to 1.0×10^{-14} mol/L and a detection limit of about 5.1×10^{-17} mol/L. The biosensor also had good reproducibility and selectivity against two-base mismatched DNA.

Tang et al. [71] discovered that ferritin has an enzyme-mimic activity derived from its ferric nanocore, and can be used to detect proteins without any other enzyme components. Note that the enzyme-mimic activity is derived from its ferric nanocore but not the protein cage. To confirm this, they used commercially available ferritin, after heating at 95 °C and complete denature of the protein cage in 8 mol/L urea, the ferric core is separated. With apoferritin as a contrast, the enzyme-mimic activity was measured using colorimetric, fluorescent, and luminescent substrates. The results revealed that the ferritin, heated ferritin and ferric core but not apoferritin had an enzyme-mimic activity on the three substrates. Further research revealed that the activity is more thermally stable and pH-tolerant than horseradish peroxidase (HRP). They also prepared antibody conjugated ferritin (streptavidin and biotin as linkage) to form a sandwich immunoassay in the

detection of nitrated human ceruloplasmin, with *N*,*N*-dimethyl-p-phenylenediamine as substrate, the detection showed a linear detection range from 33 pmol/L to 3.3 nmol/L.

With the enzyme-mimic activity of ferritin, magnetoferritin nanoparticles were able to catalyze the oxidation of peroxidase substrates 3,3,5,5-tetramethylbenzidine and diazo-aminobenzene (DAB) in the presence of H_2O_2 to give blue and brown colors, respectively. In addition, the heavy chain ferritin can bind to human cells *via* transferrin receptor 1 (TfR 1) [78]. By using these characters, Fan et al. [79] were able to detect tumor tissue with magnetoferritin nanoparticles with high sensitivity and specificity.

Lee et al. [80] used display pathogen specific antigen modified ferritin for sensitive and specific diagnostic assays of acquired immune deficiency syndrome (AIDS) and Sjögren's syndrome (SS). AIDS and SS specific antigens were genetically fused to the *C*-terminus of human ferritin heavy chain and the proteins were expressed in *Escherichia coli*. The proteins were applied to detect AIDS and SS specific antibody markers through a ferritin hydrogel. With this method, the sensitivity of the ferritin hydrogel is better than commercial ELISA kit in detecting real serum samples.

Zhao et al. [81] developed horseradish peroxidase (HRP) and apoferritin dually labeled sandwich-type electrochemical aptasensor to detect thrombin. In this assay, core/shell Fe_3O_4/Au magnetic nanoparticles (AuMNPs) were coupled with aptamer1 (Apt1) and used as recognition elements, and apoferritin dually labeled with Aptamer2 (Apt2) and HRP was used as a detection probe. The sandwich-type complex, Apt1/thrombin/Apt2-apoferritin NPs-HRP was then anchored on a screen-printed carbon electrode (SPCE). The current response to thrombin was monitored by differential pulse voltammetry (DPV). In this way the detection limit can be as low as 0.07 pmol/L.

Matrix metalloproteinases (MMPs) are a family of enzymes critical to extracellular matrix remodeling. The upregulation of MMPs is often found to be related to tumor invasiveness, metastasis, and angiogenesis [82–84]. Lin et al. [85] applied the disassembly/reassembly nature of ferritin to develop a MMP-13 activatable probe. Briefly, Cy5.5-tagged MMP-13 substrate peptide (Cy5.5-Gly-Pro-Leu-Gly-Val-Arg-Gly-Cys) and BHQ-3 (BHQ = black hole quencher) were coupled onto ferritins respectively. After adjusting the pH to 2.0, and turning back to neutral, the two forms of ferritin were coupled together. Due to the quench effect of BHQ-3 to Cy5.5, the hybrid ferritin showed much weaker fluorescence signal than the Cy5.5-peptide ferritin. Subsequently, when the probes are exposed to an MMP-rich environment, with the cleavage of MMP substrate, Cy5.5 dye molecules are released from the ferritin, and the fluorescence activity is restored. This enzyme activatable approach was also tested in other formulas for tumor detection [86–88].

5 Ferritin nanoparticles used in molecular imaging

Nanoparticles with large surface area to volume ratio facilitate surface functionalization [89–91]. Ferritin nanoparticles with unique physicochemical properties, when properly labeled, can visualize diseases through different molecular imaging modalities [92,93], such as magnetic resonance imaging (MRI), optical imaging and radionuclide imaging (positron emission tomography (PET) and single-photon emission computed tomography (SPECT)).

5.1 Ferritin nanoparticles used in disease targeting with MRI

The coupling of proton spins with larger magnetic moments, namely electronic magnetic moments, considerably speeds up the relaxation of water and provides contrast for MRI. Most commonly used MRI contrast agents are paramagnetic gadolinium ion complexes for T_1-weighted MRI and superparamagnetic magnetite particles for T_2-weighted MRI.

Ferritin is the primary intracellular iron storage protein which keeps the iron in a soluble and non-toxic form. The relaxivity of ferritin nanoparticles is strongly dependent on the amount of Fe contained in the apoferritin shell [21,94,95]. The iron nanoparticles, stored in the ferritin cages, are either in an antiferromagnetic or super paramagnetic form [96,97], which results in an unique effect on the relaxation of water as detected by MRI [98]. Ferritin is abundant in liver and spleen, thus it is possible to directly use endogenous ferritin as the reporter to monitor disease progression *in vivo* with MRI.

Choi et al. developed a model which allows tumor cells to overexpress H-ferritin by a MR reporter. This model could be used for *in vivo* tumor imaging and monitoring of lymph node metastasis [99]. The advantage of using ferritin as a MR reporter is that it does not require exogenous contrast agent to be delivered to the targeted area and makes it possible to carry out long term *in vivo* imaging [100]. Unbalance of iron homeostasis and altered level of the iron storage protein ferritin directly affect MRI contrast [101]. Clinical MRI studies have demonstrated the ability to detect changes in ferritin content in the brain, heart, liver and spleen [102], and iron accumulation in the basal ganglia in Parkinson's, Alzheimer's, Huntington's diseases [103,104].

Ferritin nanoparticles are assemblies of subunits with very narrow size distributions, which can serve as ideal templates for the synthesis of inorganic nanoparticle within the central cavity. Such nanostructures can be chemically and/or genetically modified, by redesigning the template, to impart novel functions, including targeting and

therapeutic delivery. Bennett et al. used cationized ferritin to detect thick, negatively charged basement membrane in the glomeruli of kidneys (Fig. 5) [105]. In a glomerulosclerosis model, MR with cationized ferritin, but not native ferritin, showed reduced ferritin particle accumulation in the glomeruli and diffuse accumulation in the kidney tubules, reflecting glomerular dysfunction. The same principle may be applicable to detect molecular changes in the basal membrane throughout the body.

Ferritin has hydrophobic and hydrophilic molecular channels through the protein shell. Through these molecular channels the metal core can be replaced with different metals [106–108]. Cross-linked iron oxide nanoparticles and other iron oxide formulations have been introduced into ferritin cavity. Uchida et al. characterized the MRI properties of a ferritin protein cage-iron oxide nano-composite material and investigated its use as a MRI contrast agent to label macrophages [109]. Uchida found that the macrophage uptake *in vitro* and MRI (T_2) properties of the mineralized recombinant human ferritin compare favorably with known iron oxide MRI contrast agents. In 2011, Terashima et al. [93] performed MRI (7T) of macrophages in atherosclerotic carotid arteries in streptozotocin (STZ)-induced diabetic mice. Ferritin nanoparticles encapsulated with Fe_3O_4 (25 mg Fe/kg) were intravenously injected and MRI images of both LCA and right common carotid artery (RCA) were obtained. There was neither T_2* signal loss in the control RCA nor in artery in sham, but a clear loss in the macrophage-rich ligated LCA (Fig. 6). Quantitative analysis showed that the T_2*-induced reduction in lumen contrast was significant at both 24 and 48 h in the ligated LCA compared to contralateral RCA and sham controls. Immunohistochemical experiments also confirmed that ferritin nanoparticles were co-localized with macrophages in the neointima of the ligated LCA but not in the RCA or sham-operated arteries.

As described before, MMPs are engaged in the degradation of extracellular matrices and are tightly associated with malignant processes of tumors, including metastasis and angiogenesis. Particularly, MMP-2 has been identified as one of the key MMPs. MMP-2 belongs to a category of type IV collagenases and plays a critical role in the degradation of basement membranes [110,111]. Matsumura et al. [112] reported a modified ferritin as a MMP-2 responsive nanocarrier. The designed ferritin contained a triad of modifiers composed of four parts (from inner to outside): 1) ferritin, 2) hydrophobic segment, 3) linker segment, 4) hydrophilic polyethylene glycol segment. The linker segment is MMP-2 substrate that can be cleaved by the protease and then the hydrophobic segments are exposed, resulting in aggregation of ferritin cages and enhancement of T_2 relaxivity.

Gadolinium (Gd) ion is a well-known T_1-shortening reagent, because Gd possesses seven unpaired electrons [113]. One obvious advantage of T_1 imaging over T_2 imaging is the reduced T_1 caused by the contrast agent leads to a positive contrast on a T_1 map [92]. Gd encapsulation within ferritin cage represents a different approach to the development of MRI contrast agents.

Sanchez et al. [114] prepared water-soluble gadolinium oxide (Gd_2O_3) nanoparticles within apoferritin. Based on

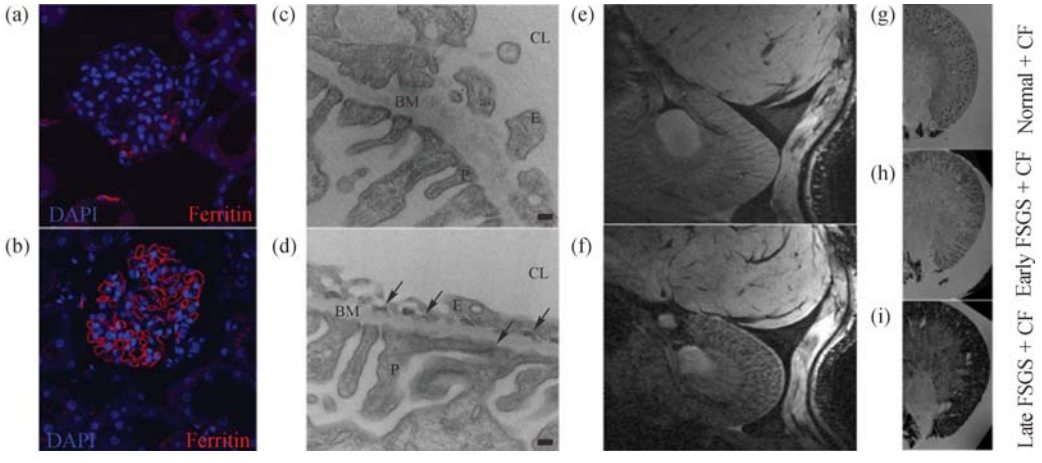

Fig. 5 Basement membrane detection in kidney glomeruli. (a,b) Immunofluorescence microscopy (40×) showing the accumulation of systemically injected cationized ferritin (CF) (b) in glomerular basement membrane of rat kidneys and little accumulation of native ferritin (NF) (a); (c,d) transmission electron microscopy of normal rat kidney glomeruli after three systemic injection of NF (c) and CF (d). Scale bars = 100 nm; (e,f) respiratory-gated MRI (GRE) detection of CF after intravenous injection: (e) GRE image of a rat kidney after five NF injections, showing darkening of the MRI signal due to blood vessels in the cortex and medulla. (f) GRE image of a rat kidney after five injections of CF, showing darkening of glomeruli in the cortex due to accumulation of CF; (g,h,i) detection of glomerular injury in puromycin-induced focal segmental glomerulosclerosis (FSGS) by GRE MRI with CF. The accumulation of CF showed a clear spotted distribution in glomeruli from normal kidney (g), the spots were surrounded by areas of signal hypointensity but still visible in cortex of kidney from early FSGS (h) at day 13 after puromycin aminonucleoside (PAN) injection, and then cortical signal was darkened without visible spots in kidneys of late FSGS (i) 13 weeks after PAN injection in an *ex vivo* study. Adapted from ref. [105] with permission

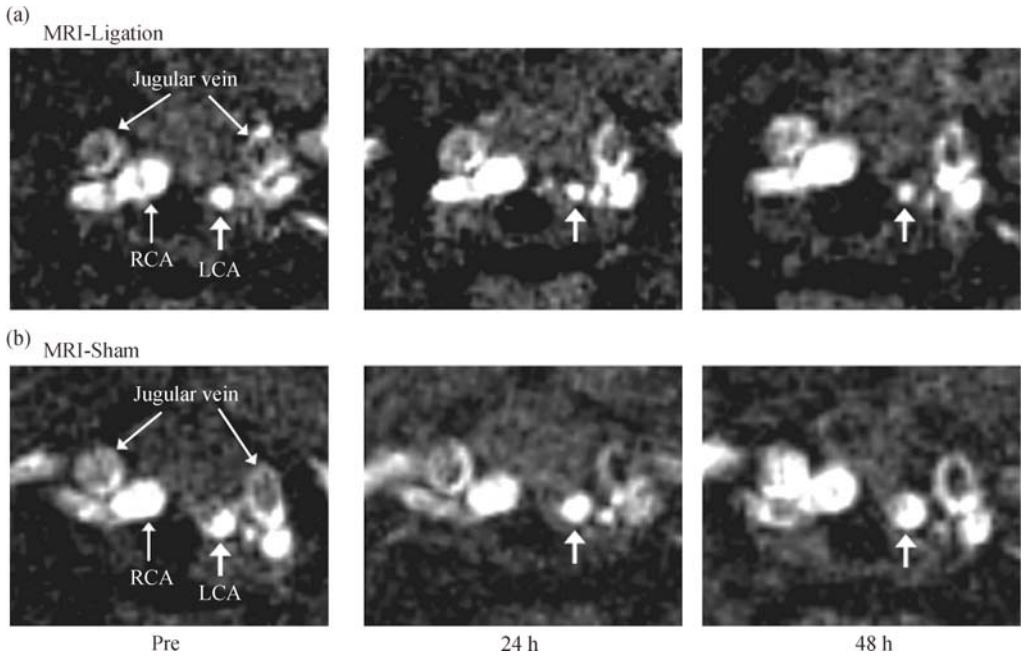

Fig. 6 *In vivo* MRI of carotid arteries in ligated and sham-operated mice with magnetite mineralized heavy-chain ferritin (HFn-Fe_3O_4). (a) The ligated left carotid artery (LCA) is smaller than the non-ligated right carotid artery (RCA) prior to contrast injection. Concentric signal loss was found in the LCA lumen at 24 and 48 h after HFn-Fe_3O_4 injection but not for the RCA; (b) no change was seen in the sham-operated LCA. Adapted from ref. [93] with permission

the Gd/apoferritin concentration ratio, each apoferritin would have 1700 Gd. The successfully built ferritin nanoparticles with NMR longitudinal and transverse relaxivities about 10 and 70 times higher than those of clinically approved paramagnetic Gd-chelates. It is also of note that the r_2/r_1 ratio changes in response to frequency. Makino et al. was also able to encapsulate a cationic Gd chelate, Gd-Me_2DOTA, into apoferritin by electrostatic interactions. Immobilization of Gd chelate on the inner surface prevents the excess shortening of the T_2 relaxation time and increases T_1 relaxivity by one order of magnitude compared to the free metal chelate. Further decorating the apoferritin surface with dextran led to tumor contrast after intravenous administration based on EPR effect.

5.2 Ferritin nanoparticles used in multimodal imaging

Multimodality imaging is drawing more and more attention and gaining popularity [115–118]. The basic principle arises from the notion of improving the quality and accuracy of disease management by combining different but complementary strengths of multiple imaging techniques. The development of PET/CT is a good example of fused technique that permits simultaneous acquisition of functional and high-resolution anatomical information [119–121]. Similarly, the assembly of near-infrared fluorescence (NIRF) imaging and PET is also a useful combination, since it provides both *in vivo* imaging interrogation and *ex vivo* validation so as to minimize the chances of misdiagnosis [122–124]. Ferritin cage can serve as a multifunctional platform for the loading of metal nanoparticles and can be engineered for use as a cell-specific targeting moiety. Cell-targeting moieties can be exposed on the exterior surface of protein cage architectures by means of both genetic and chemical modifications [7,125,126].

Lin et al. [16] developed chimeric ferritin nanoparticles for multimodal tumor imaging (Fig. 7). RGD4C peptide was genetically fused to the *N*-terminus of ferritin for integrin $\alpha_v\beta_3$ targeting. Fluorescence dye (Cy5.5) was chemically coupled to the ferritin surface for NIRF imaging and ^{64}Cu was encapsulated in ferritin interiors by association with metal binding sites for PET imaging. With this multifunctional loading strategy, the interference among different docked motifs is negligible. The similar approach can be applied to develop different multi-functional contrast agents for different combinations of imaging modalities.

Recently, we also successfully prepared copper sulfide nanoparticles within the cavity of ferritin using a biomimetic synthesis method for cancer theranostics (Fig. 8) [118]. Such uniform ferritin nanoparticles with copper sulfide inside showed strong near-infrared absorbance and high photothermal conversion yield. With the involvement of $^{64}Cu^{2+}$ in the synthesis process, both photoacoustic imaging (PAI) and PET imaging were successfully carried out for pharmacokinetics and biodistribution analyses at the same time. The combination of

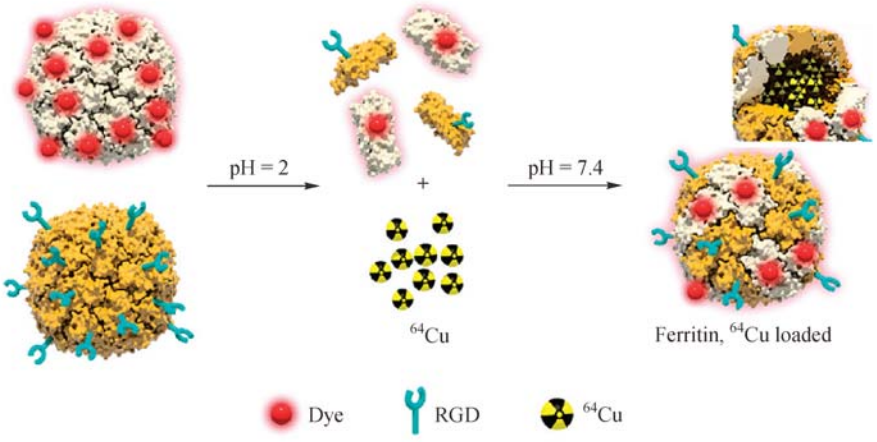

Fig. 7 Illustration of the process of triple loading of chimeric ferritin nanoparticles. RGD4C peptide is genetically fused to the *N*-terminus of ferritin, Cy5.5 is coupled to the protein surface *via* standard EDC-NHS chemistry. At acidic pH, RGD4C-ferritin and Cy5.5-ferritin conjugates are mixed and broken into individual subunits, which were radiolabeled with 64Cu and then reconstituted into chimeric ferritin nanocages that contain both RGD peptide and Cy5.5 fluorophore on the surface and radioisotope in the cavity. Adapted from ref. [16] with permission

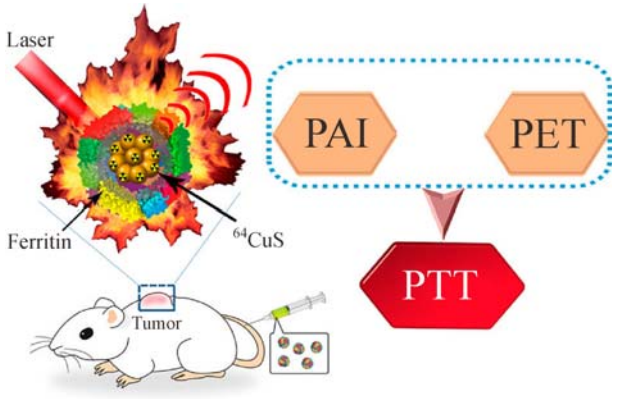

Fig. 8 Schematic illustration of copper sulfide-ferritin nanoparticle were radiolabeled with ^{64}Cu and used for photoacoustic and PET imaging guided photothermal therapy agent. Adapted from ref. [118] with permission

PAI and PET facilitates noninvasive, highly sensitive, and quantitative *in vivo* measurement of particle distribution. Additionally, with the high photothermal conversion efficiency, copper sulfide-ferritin nanoparticles were applied to photothermal therapy with good biocompatibility.

One of the most difficult issues that limit clinical translation of ferritin nanoparticles is the detailed understanding of their behavior after administration into the body [118,127]. Interestingly, PET provides a powerful way to visualize the biodistribution of ^{64}Cu-labeled ferritin in mice. As expected, ferritin nanoparticles were mainly found in the liver and digestive system after injection, and it showed an increased tumor accumulation within first 8 h post-injection, and then plateaued until 24 h time point (Fig. 9). However, the safety profile including pharmacology and toxicology should be studied in more details prior to the possible application this material in human.

6 Conclusions

Ferritin nanoparticle-based bioapplications have attracted much attention in different fields. It is straightforward to develop *in vitro* diagnostic agents using ferritin with high sensitivity and specificity [79]. For *in vivo* applications, however, the efforts have been focused on enhancing efficacy, biocompatibility and pharmacokinetic profile of the current ferritin-based delivery systems [127]. Several barriers remain in the process of clinical translation, including the difficulty of mass production, as well as limited knowledge of pharmacology and toxicology data.

Overall, ferritin nanocage has been widely used as a platform to prepare different metallic nanoparticles and

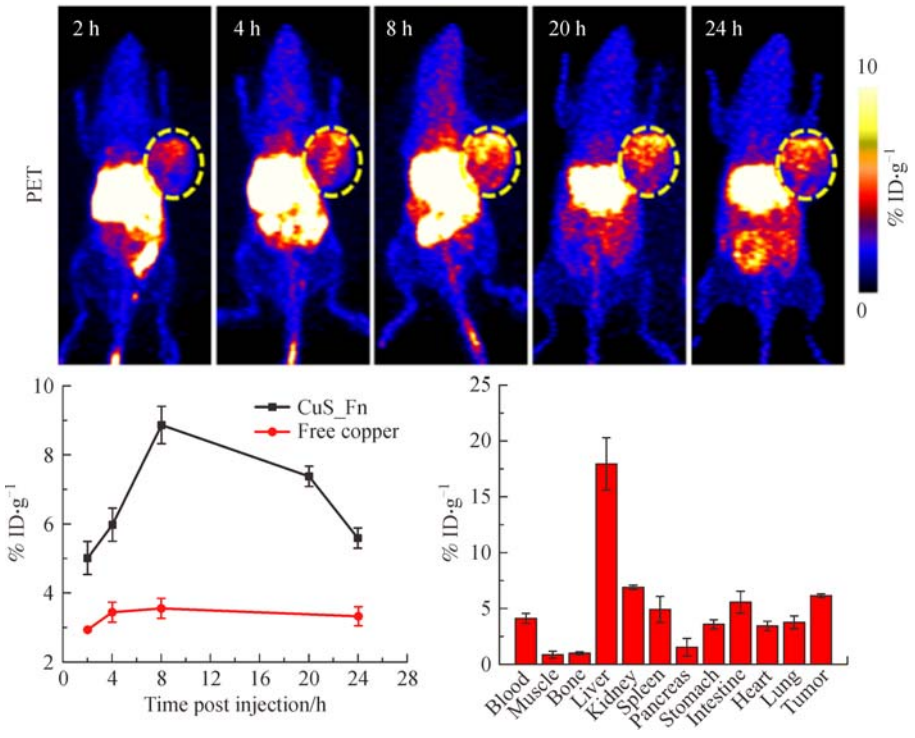

Fig. 9 Biodistribution of ^{64}Cu-labeled ferritin nanoparticles in U87MG tumor-bearing mice after intravenous injection. Adapted from ref. [118] with permission

offer ample opportunities for external functionalization for biomedical applications. With its unique characteristics, including commonly found in almost organism, very low toxicity, easy modification by genetic and chemical methods, large loading rate, ferritin nanoparticles have high potential in drug delivery, bioassay, disease diagnosis and therapy. Ferritin nanoparticles with more targeted specific targeting motifs can lead to more effective diagnosis and therapy of diseases. More translational work based on ferritin nanoparticles are expected in the foreseeable future.

Acknowledgements This work was supported by the Major State Basic Research Development Program of China (973 Program) (Grant Nos. 2014CB744503 and 2013CB733802), the National Natural Science Foundation of China (NSFC) (Grant Nos. 81422023, 81371596, 51273165, and U1505221), the Fundamental Research Funds for the Central Universities (Grant Nos. 20720160065 and 20720150141), the Science Foundation of Fujian Province (No. 2014Y2004), and the Program for New Century Excellent Talents in University, China (NCET-13-0502), and the Intramural Research Program (IRP), National Institute of Biomedical Imaging and Bioengineering (NIBIB), National Institutes of Health (NIH). Dr. Zhantong Wang was particially funded by the China Scholarship Council (CSC).

Conflicts of Interest The authors declare no competing financial interest.

References

1. Worwood M, Cook J D. Serum ferritin. Critical Reviews in Clinical Laboratory Sciences, 1979, 10(2): 171–204
2. Meldrum F C, Heywood B R, Mann S. Magnetoferritin: *In vitro* synthesis of a novel magnetic protein. Science, 1992, 257(5069): 522–523
3. Zeth K, Hoiczyk E, Okuda M. Ferroxidase-mediated iron oxide biomineralization: Novel pathways to multifunctional nanoparticles. Trends in Biochemical Sciences, 2016, 41(2): 190–203
4. Chasteen N D, Harrison P M. Mineralization in ferritin: An efficient means of iron storage. Journal of Structural Biology, 1999, 126(3): 182–194
5. Uchida M, Kang S, Reichhardt C, Harlen K, Douglas T. The ferritin superfamily: Supramolecular templates for materials synthesis. Biochimica et Biophysica Acta, 2010, 1800(8): 834–845
6. Bulte J W, Douglas T, Mann S, Frankel R B, Moskowitz B M, Brooks R A, Baumgarner C D, Vymazal J, Strub M P, Frank J A. Magnetoferritin: Characterization of a novel superparamagnetic MR contrast agent. Journal of Magnetic Resonance Imaging, 1994, 4(3): 497–505
7. Uchida M, Flenniken M L, Allen M, Willits D A, Crowley B E, Brumfield S, Willis A F, Jackiw L, Jutila M, Young M J, Douglas T. Targeting of cancer cells with ferrimagnetic ferritin cage nanoparticles. Journal of the American Chemical Society, 2006, 128(51): 16626–16633
8. Okuda M, Iwahori K, Yamashita I, Yoshimura H. Fabrication of nickel and chromium nanoparticles using the protein cage of apoferritin. Biotechnology and Bioengineering, 2003, 84(2): 187–194
9. Galvez N, Sanchez P, Dominguez-Vera J M. Preparation of Cu and

CuFe prussian blue derivative nanoparticles using the apoferritin cavity as nanoreactor. Dalton Transactions (Cambridge, England), 2005, 15(15): 2492–2494

10. Jeong G H, Yamazaki A, Suzuki S, Yoshimura H, Kobayashi Y, Homma Y. Cobalt-filled apoferritin for suspended single-walled carbon nanotube growth with narrow diameter distribution. Journal of the American Chemical Society, 2005, 127(23): 8238–8239
11. Fan R, Chew S W, Cheong V V, Orner B P. Fabrication of gold nanoparticles inside unmodified horse spleen apoferritin. Small, 2010, 6(14): 1483–1487
12. Zhen Z, Tang W, Chen H, Lin X, Todd T, Wang G, Cowger T, Chen X, Xie J. RGD-modified apoferritin nanoparticles for efficient drug delivery to tumors. ACS Nano, 2013, 7(6): 4830–4837
13. Zhen Z, Tang W, Guo C, Chen H, Lin X, Liu G, Fei B, Chen X, Xu B, Xie J. Ferritin nanocages to encapsulate and deliver photosensitizers for efficient photodynamic therapy against cancer. ACS Nano, 2013, 7(8): 6988–6996
14. Tian Y, Yan X, Saha M L, Niu Z, Stang P J. Hierarchical self-assembly of responsive organoplatinum(ii) metallacycle-TMV complexes with turn-on fluorescence. Journal of the American Chemical Society, 2016, 138(37): 12033–12036
15. Harrison P M, Arosio P. The ferritins: Molecular properties, iron storage function and cellular regulation. Biochimica et Biophysica Acta, 1996, 1275(3): 161–203
16. Lin X, Xie J, Niu G, Zhang F, Gao H, Yang M, Quan Q, Aronova M A, Zhang G, Lee S, et al. Chimeric ferritin nanocages for multiple function loading and multimodal imaging. Nano Letters, 2011, 11(2): 814–819
17. Yamashita I, Iwahori K, Kumagai S. Ferritin in the field of nanodevices. Biochimica et Biophysica Acta, 2010, 1800(8): 846–857
18. Jolley C C, Uchida M, Reichhardt C, Harrington R, Kang S, Klem M T, Parise J B, Douglas T. Size and crystallinity in protein-templated inorganic nanoparticles. Chemistry of Materials, 2010, 22(16): 4612–4618
19. Zhang L, Swift J, Butts C A, Yerubandi V, Dmochowski I J. Structure and activity of apoferritin-stabilized gold nanoparticles. Journal of Inorganic Biochemistry, 2007, 101(11-12): 1719–1729
20. Rother M, Nussbaumer M G, Renggli K, Bruns N. Protein cages and synthetic polymers: A fruitful symbiosis for drug delivery applications, bionanotechnology and materials science. Chemical Society Reviews, 2016, 45(22): 6213–6249
21. Ghirlando R, Mutskova R, Schwartz C. Enrichment and characterization of ferritin for nanomaterial applications. Nanotechnology, 2016, 27(4): 045102
22. Konijn A, Meyron-Holtz E, Levy R, Ben-Bassat H, Matzner Y. Specific binding of placental acidic isoferritin to cells of the T-cell line HD-MAR. FEBS Letters, 1990, 263(2): 229–232
23. Bretscher M S, Thomson J N. Distribution of ferritin receptors and coated pits on giant Hela cells. EMBO Journal, 1983, 2(4): 599–603
24. Lei Y, Hamada Y, Li J, Cong L, Wang N, Li Y, Zheng W, Jiang X. Targeted tumor delivery and controlled release of neuronal drugs with ferritin nanoparticles to regulate pancreatic cancer progression. Journal of Controlled Release, 2016, 232: 131–142
25. Zhao Y, Liang M, Li X, Fan K, Xiao J, Li Y, Shi H, Wang F, Choi H S, Cheng D, et al. Bioengineered magnetoferritin nanoprobes for single-dose nuclear-magnetic resonance tumor imaging. ACS Nano, 2016, 10(4): 4184–4191
26. Adams P C, Powell L W, Halliday J W. Isolation of a human hepatic ferritin receptor. Hepatology (Baltimore, MD.), 1988, 8(4): 719–721
27. Chen X. Multimodality imaging of tumor integrin alphavbeta3 expression. Mini-Reviews in Medicinal Chemistry, 2006, 6(2): 227–233
28. Liu Y, Wang Z, Zhang H, Lang L, Ma Y, He Q, Lu N, Huang P, Song J, Liu Z, et al. A photothermally responsive nanoprobe for bioimaging based on edman degradation. Nanoscale, 2016, 8(20): 10553–10557
29. Kitagawa T, Kosuge H, Uchida M, Dua M M, Iida Y, Dalman R L, Douglas T, McConnell M V. Rgd-conjugated human ferritin nanoparticles for imaging vascular inflammation and angiogenesis in experimental carotid and aortic disease. Molecular Imaging & Biology, 2012, 14(3): 315–324
30. Choi H S, Nasr K, Alyabyev S, Feith D, Lee J H, Kim S H, Ashitate Y, Hyun H, Patonay G, Strekowski L, et al. Synthesis and *in vivo* fate of zwitterionic near—infrared fluorophores. Angewandte Chemie International Edition, 2011, 50(28): 6258–6263
31. Agostinis P, Berg K, Cengel K A, Foster T H, Girotti A W, Gollnick S O, Hahn S M, Hamblin M R, Juzeniene A, Kessel D, et al. Photodynamic therapy of cancer: An update. CA: a Cancer Journal for Clinicians, 2011, 61(4): 250–281
32. Ochsner M. Photophysical and photobiological processes in the photodynamic therapy of tumours. Journal of Photochemistry and Photobiology. B, Biology, 1997, 39(1): 1–18
33. Brown S B, Brown E A, Walker I. The present and future role of photodynamic therapy in cancer treatment. Lancet Oncology, 2004, 5(8): 497–508
34. Cairnduff F, Stringer M R, Hudson E J, Ash D V, Brown S B. Superficial photodynamic therapy with topical 5-aminolaevulinic acid for superficial primary and secondary skin cancer. British Journal of Cancer, 1994, 69(3): 605–608
35. Falvo E, Tremante E, Fraioli R, Leonetti C, Zamparelli C, Boffi A, Morea V, Ceci P, Giacomini P. Antibody-drug conjugates: Targeting melanoma with cisplatin encapsulated in protein-cage nanoparticles based on human ferritin. Nanoscale, 2013, 5(24): 12278–12285
36. MacKie R. Melanoma prevention and early detection. British Medical Bulletin, 1995, 51(3): 570–583
37. Siegel R, Naishadham D, Jemal A. Cancer statistics, 2012. CA: a Cancer Journal for Clinicians, 2012, 62(1): 10–29
38. Greenlee R T, Murray T, Bolden S, Wingo P A. Cancer statistics, 2000. CA: a Cancer Journal for Clinicians, 2000, 50(1): 7–33
39. Rigel D S, Carucci J A. Malignant melanoma: Prevention, early detection, and treatment in the 21st century. CA: a Cancer Journal for Clinicians, 2000, 50(4): 215–236
40. Morgenstern D A, Asher R A, Fawcett J W. Chondroitin sulphate proteoglycans in the CNS injury response. Progress in Brain Research, 2002, 137: 313–332

41. Eisenmann K M, McCarthy J B, Simpson M A, Keely P J, Guan J L, Tachibana K, Lim L, Manser E, Furcht L T, Iida J. Melanoma chondroitin sulphate proteoglycan regulates cell spreading through Cdc42, Ack-1 and p130cas. Nature Cell Biology, 1999, 1(8): 507–513
42. Thon N, Haas C A, Rauch U, Merten T, Fässler R, Frotscher M, Deller T. The chondroitin sulphate proteoglycan brevican is upregulated by astrocytes after entorhinal cortex lesions in adult rats. European Journal of Neuroscience, 2000, 12(7): 2547–2558
43. Levine J, Nishiyama A. The NG2 chondroitin sulfate proteoglycan: A multifunctional proteoglycan associated with immature cells. Perspectives on Developmental Neurobiology, 1996, 3(4): 245–259
44. Oohira A, Matsui F, Watanabe E, Kushima Y, Maeda N. Developmentally regulated expression of a brain specific species of chondroitin sulfate proteoglycan, neurocan, identified with a monoclonal antibody LG2 in the rat cerebrum. Neuroscience, 1994, 60(1): 145–157
45. Levine J M, Stallcup W B. Plasticity of developing cerebellar cells *in vitro* studied with antibodies against the NG2 antigen. Journal of Neuroscience, 1987, 7(9): 2721–2731
46. Maeda H, Wu J, Sawa T, Matsumura Y, Hori K. Tumor vascular permeability and the EPR effect in macromolecular therapeutics: A review. Journal of Controlled Release, 2000, 65(1): 271–284
47. Mamo T, Poland G A. Nanovaccinology: The next generation of vaccines meets 21st century materials science and engineering. Vaccine, 2012, 30(47): 6609–6611
48. des Rieux A, Fievez V, Garinot M, Schneider Y J, Préat V. Nanoparticles as potential oral delivery systems of proteins and vaccines: A mechanistic approach. Journal of Controlled Release, 2006, 116(1): 1–27
49. Singh M, Chakrapani A, O'Hagan D. Nanoparticles and microparticles as vaccine-delivery systems. Expert Review of Vaccines, 2007, 6(5): 797–808
50. Oyewumi M O, Kumar A, Cui Z. Nano-microparticles as immune adjuvants: Correlating particle sizes and the resultant immune responses. Expert Review of Vaccines, 2010, 9(9): 1095–1107
51. Zhao L, Seth A, Wibowo N, Zhao C X, Mitter N, Yu C, Middelberg A P. Nanoparticle vaccines. Vaccine, 2014, 32(3): 327–337
52. Zhao K, Chen G, Shi X, Gao T, Li W, Zhao Y, Zhang F, Wu J, Cui X, Wang Y F. Preparation and efficacy of a live newcastle disease virus vaccine encapsulated in chitosan nanoparticles. PLoS One, 2012, 7(12): e53314
53. Borges O, Cordeiro-da-Silva A, Tavares J, Santarém N, de Sousa A, Borchard G, Junginger H E. Immune response by nasal delivery of hepatitis B surface antigen and codelivery of a CpG ODN in alginate coated chitosan nanoparticles. European Journal of Pharmaceutics and Biopharmaceutics, 2008, 69(2): 405–416
54. Nochi T, Yuki Y, Takahashi H, Sawada S, Mejima M, Kohda T, Harada N, Kong I G, Sato A, Kataoka N, et al. Nanogel antigenic protein-delivery system for adjuvant-free intranasal vaccines. Nature Materials, 2010, 9(7): 572–578
55. Stone J W, Thornburg N J, Blum D L, Kuhn S J, Wright D W, Crowe J E Jr. Gold nanorod vaccine for respiratory syncytial virus. Nanotechnology, 2013, 24(29): 295102
56. Wang T, Zou M, Jiang H, Ji Z, Gao P, Cheng G. Synthesis of a novel kind of carbon nanoparticle with large mesopores and macropores and its application as an oral vaccine adjuvant. European Journal of Pharmaceutical Sciences, 2011, 44(5): 653–659
57. Glück R, Moser C, Metcalfe I C. Influenza virosomes as an efficient system for adjuvanted vaccine delivery. Expert Opinion on Biological Therapy, 2004, 4(7): 1139–1145
58. Zhu F C, Zhang J, Zhang X F, Zhou C, Wang Z Z, Huang S J, Wang H, Yang C L, Jiang H M, Cai J P, et al. Efficacy and safety of a recombinant hepatitise vaccine in healthy adults: A large-scale, randomised, double-blind placebo-controlled, phase 3 trial. Lancet, 2010, 376(9744): 895–902
59. Sliepen K, Ozorowski G, Burger J A, van Montfort T, Stunnenberg M, LaBranche C, Montefiori D C, Moore J P, Ward A B, Sanders R W. Presenting native-like HIV-1 envelope trimers on ferritin nanoparticles improves their immunogenicity. Retrovirology, 2015, 12(82): 15–21
60. Champion C I, Kickhoefer V A, Liu G, Moniz R J, Freed A S, Bergmann L L, Vaccari D, Raval-Fernandes S, Chan A M, Rome L H, Kelly K A. A vault nanoparticle vaccine induces protective mucosal immunity. PLoS One, 2009, 4(4): e5409
61. Kanekiyo M, Wei C J, Yassine H M, McTamney P M, Boyington J C, Whittle J R, Rao S S, Kong W P, Wang L, Nabel G J. Self-assembling influenza nanoparticle vaccines elicit broadly neutralizing H1N1 antibodies. Nature, 2013, 499(7456): 102–106
62. Cho K J, Shin H J, Lee J H, Kim K J, Park S S, Lee Y, Lee C, Park S S, Kim K H. The crystal structure of ferritin from helicobacter pylori reveals unusual conformational changes for iron uptake. Journal of Molecular Biology, 2009, 390(1): 83–98
63. Steinman R M. Decisions about dendritic cells: Past, present, and future. Annual Review of Immunology, 2012, 30(1): 1–22
64. Gilboa E. DC-based cancer vaccines. Journal of Clinical Investigation, 2007, 117(5): 1195–1203
65. Aarntzen E, Figdor C, Adema G, Punt C, De Vries I. Dendritic cell vaccination and immune monitoring. Cancer Immunology, Immunotherapy, 2008, 57(10): 1559–1568
66. Han J A, Kang Y J, Shin C, Ra J S, Shin H H, Hong S Y, Do Y, Kang S. Ferritin protein cage nanoparticles as versatile antigen delivery nanoplatforms for dendritic cell (DC)-based vaccine development. Nanomedicine; Nanotechnology, Biology, and Medicine, 2013, 10(3): 561–569
67. Shimonkevitz R, Colon S, Kappler J W, Marrack P, Grey H M. Antigen recognition by H-2-restricted T cells. II. A tryptic ovalbumin peptide that substitutes for processed antigen. Journal of Immunology (Baltimore, MD: 1950), 1984, 133(4): 2067–2074
68. Liu D, Wang Z, Jin A, Huang X, Sun X, Wang F, Yan Q, Ge S, Xia N, Niu G, Liu G, Hight Walker A R, Chen X. Acetylcholinesterase—catalyzed hydrolysis allows ultrasensitive detection of pathogens with the naked eye. Angewandte Chemie International Edition in English, 2013, 52(52): 14065–14069
69. Lee S H, Lee H, Park J S, Choi H, Han K Y, Seo H S, Ahn K Y, Han S S, Cho Y, Lee K H, et al. A novel approach to ultrasensitive diagnosis using supramolecular protein nanoparticles. FASEB Journal, 2007, 21(7): 1324–1334

70. Abbaspour A, Noori A. Electrochemical detection of individual single nucleotide polymorphisms using monobase-modified apoferritin-encapsulated nanoparticles. Biosensors & Bioelectronics, 2012, 37(1): 11–18
71. Tang Z, Wu H, Zhang Y, Li Z, Lin Y. Enzyme-mimic activity of ferric nano-core residing in ferritin and its biosensing applications. Analytical Chemistry, 2011, 83(22): 8611–8616
72. Men D, Zhang T T, Hou L W, Zhou J, Zhang Z P, Shi Y Y, Zhang J L, Cui Z Q, Deng J Y, Wang D B, et al. Self-assembly of ferritin nanoparticles into an enzyme nanocomposite with tunable size for ultrasensitive immunoassay. ACS Nano, 2015, 9(11): 10852–10860
73. Liu G, Wang J, Wu H, Lin Y. Versatile apoferritin nanoparticle labels for assay of protein. Analytical Chemistry, 2006, 78(21): 7417–7423
74. Liu G, Wu H, Wang J, Lin Y. Apoferritin-templated synthesis of metal phosphate nanoparticle labels for electrochemical immunoassay. Small, 2006, 2(10): 1139–1143
75. Beutler B, Cerami A. Cachectin and tumour necrosis factor as two sides of the same biological coin. Nature, 1986, 320(6063): 584–588
76. Scuderi P, Lam K, Ryan K, Petersen E, Sterling K, Finley P, Ray C G, Slymen D, Salmon S. Raised serum levels of tumour necrosis factor in parasitic infections. Lancet, 1986, 328(8520): 1364–1365
77. Yu F, Li G, Qu B, Cao W. Electrochemical detection of DNA hybridization based on signal DNA probe modified with Au and apoferritin nanoparticles. Biosensors & Bioelectronics, 2010, 26 (3): 1114–1117
78. Li L, Fang C J, Ryan J C, Niemi E C, Lebrón J A, Björkman P J, Arase H, Torti F M, Torti S V, Nakamura M C, et al. Binding and uptake of H-ferritin are mediated by human transferrin receptor-1. Proceedings of the National Academy of Sciences of the United States of America, 2010, 107(8): 3505–3510
79. Fan K, Cao C, Pan Y, Lu D, Yang D, Feng J, Song L, Liang M, Yan X. Magnetoferritin nanoparticles for targeting and visualizing tumour tissues. Nature Nanotechnology, 2012, 7(7): 459–464
80. Lee E J, Ahn K Y, Lee J H, Park J S, Song J A, Sim S J, Lee E B, Cha Y J, Lee J. A novel bioassay platform using ferritin-based nanoprobe hydrogel. Advanced Materials, 2012, 24(35): 4739–4744
81. Zhao J, Liu M, Zhang Y, Li H, Lin Y, Yao S. Apoferritin protein nanoparticles dually-labeled with aptamer and HRP as a sensing probe for thrombin detection. Analytica Chimica Acta, 2012, 1 (759): 53–60
82. John A, Tuszynski G. The role of matrix metalloproteinases in tumor angiogenesis and tumor metastasis. Pathology Oncology Research, 2001, 7(1): 14–23
83. Stetler-Stevenson W G, Aznavoorian S, Liotta L A. Tumor cell interactions with the extracellular matrix during invasion and metastasis. Annual Review of Cell Biology, 1993, 9(1): 541–573
84. Malemud C J. Matrix metalloproteinases (MMPs) in health and disease: An overview. Frontiers in Bioscience: A Journal and Virtual Library, 2006, 11: 1696
85. Lin X, Xie J, Zhu L, Lee S, Niu G, Ma Y, Kim K, Chen X. Hybrid ferritin nanoparticles as activatable probes for tumor imaging. Angewandte Chemie International Edition in English, 2011, 50(7): 1569–1572
86. Zhu L, Ma Y, Kiesewetter D O, Wang Y, Lang L, Lee S, Niu G, Chen X. Rational design of matrix metalloproteinase-13 activatable probes for enhanced specificity. ACS Chemical Biology, 2013, 9(2): 510–516
87. Zhu L, Xie J, Swierczewska M, Zhang F, Quan Q, Ma Y, Fang X, Kim K, Lee S, Chen X. Real-time video imaging of protease expression *in vivo*. Theranostics, 2011, 1: 18–27
88. Wang J, Zhang L, Chen M, Gao S, Zhu L. Activatable ferritin nanocomplex for real-time monitoring of caspase-3 activation during photodynamic therapy. ACS Applied Materials & Interfaces, 2015, 7(41): 23248–23256
89. Choi S H, Na H B, Park Y I, An K, Kwon S G, Jang Y, Park M H, Moon J, Son J S, Song I C, et al. Simple and generalized synthesis of oxide-metal heterostructured nanoparticles and their applications in multimodal biomedical probes. Journal of the American Chemical Society, 2008, 130(46): 15573–15580
90. Wang H, Cao F, De A, Cao Y, Contag C, Gambhir S S, Wu J C, Chen X. Trafficking mesenchymal stem cell engraftment and differentiation in tumor-bearing mice by bioluminescence imaging. Stem Cells (Dayton, OH), 2009, 27(7): 1548–1558
91. Xu C, Yuan Z, Kohler N, Kim J, Chung M A, Sun S. Fept nanoparticles as an Fe reservoir for controlled Fe release and tumor inhibition. Journal of the American Chemical Society, 2009, 131 (42): 15346–15351
92. Bhirde A, Xie J, Swierczewska M, Chen X. Nanoparticles for cell labeling. Nanoscale, 2011, 3(1): 142–153
93. Terashima M, Uchida M, Kosuge H, Tsao P S, Young M J, Conolly S M, Douglas T, McConnell M V. Human ferritin cages for imaging vascular macrophages. Biomaterials, 2011, 32(5): 1430–1437
94. Mills P H, Ahrens E T. Theoretical MRI contrast model for exogenous T2 agents. Magnetic Resonance in Medicine, 2007, 57 (2): 442–447
95. Charlton J R, Pearl V M, Denotti A R, Lee J B, Swaminathan S, Scindia Y M, Charlton N P, Baldelomar E J, Beeman S C, Bennett K M. Biocompatibility of ferritin-based nanoparticles as targeted mri contrast agents. Nanomedicine; Nanotechnology, Biology, and Medicine, 2016, 12(6): 1735–1745
96. Domínguez-Vera J M, Fernandez B, Galvez N. Native and synthetic ferritins for nanobiomedical applications: Recent advances and new perspectives. Future Medicinal Chemistry, 2010, 2(4): 609–618
97. Maraloiu V A, Appaix F, Broisat A, Le Guellec D, Teodorescu V S, Ghezzi C, van der Sanden B, Blanchin M G. Multiscale investigation of uspio nanoparticles in atherosclerotic plaques and their catabolism and storage *in vivo*. Nanomedicine; Nanotechnology, Biology, and Medicine, 2016, 12(1): 191–200
98. Xie H, Cheng Y C, Kokeny P, Liu S, Hsieh C Y, Haacke E M, Palihawadana Arachchige M, Lawes G. A quantitative study of susceptibility and additional frequency shift of three common materials in MRI. Magnetic Resonance in Medicine, 2016, 76(4): 1263–1269
99. Choi S H, Cho H R, Kim H S, Kim Y H, Kang K W, Kim H, Moon

W K. Imaging and quantification of metastatic melanoma cells in lymph nodes with a ferritin MR reporter in living mice. NMR in Biomedicine, 2012, 25(5): 737–745

100. Fan K, Gao L, Yan X. Human ferritin for tumor detection and therapy. Wiley Interdisciplinary Reviews. Nanomedicine and Nanobiotechnology, 2013, 5(4): 287–298
101. Schenck J F, Zimmerman E A. High-field magnetic resonance imaging of brain iron: Birth of a biomarker? NMR in Biomedicine, 2004, 17(7): 433–445
102. Christoforidis A, Haritandi A, Tsitouridis I, Tsatra I, Tsantali H, Karyda S, Dimitriadis A S, Athanassiou-Metaxa M. Correlative study of iron accumulation in liver, myocardium, and pituitary assessed with MRI in young thalassemic patients. Journal of Pediatric Hematology/Oncology, 2006, 28(5): 311–315
103. Bartzokis G, Cummings J L, Markham C H, Marmarelis P Z, Treciokas L J, Tishler T A, Marder S R, Mintz J. MRI evaluation of brain iron in earlier-and later-onset Parkinson's disease and normal subjects. Magnetic Resonance Imaging, 1999, 17(2): 213–222
104. Bartzokis G, Tishler T. MRI evaluation of basal ganglia ferritin iron and neurotoxicity in Alzheimer's and Huntingon's disease. Cellular and Molecular Biology, 2000, 46(4): 821–833
105. Bennett K M, Zhou H, Sumner J P, Dodd S J, Bouraoud N, Doi K, Star R A, Koretsky A P. MRI of the basement membrane using charged nanoparticles as contrast agents. Magnetic Resonance in Medicine, 2008, 60(3): 564–574
106. Kim J W, Choi S H, Lillehei P T, Chu S H, King G C, Watt G D. Cobalt oxide hollow nanoparticles derived by bio-templating. Chemical Communications, 2005, (32): 4101–4103
107. Deng Q Y, Yang B, Wang J F, Whiteley C G, Wang X N. Biological synthesis of platinum nanoparticles with apoferritin. Biotechnology Letters, 2009, 31(10): 1505–1509
108. Sun C, Yang H, Yuan Y, Tian X, Wang L, Guo Y, Xu L, Lei J, Gao N, Anderson G J, et al. Controlling assembly of paired gold clusters within apoferritin nanoreactor for *in vivo* kidney targeting and biomedical imaging. Journal of the American Chemical Society, 2011, 133(22): 8617–8624
109. Uchida M, Terashima M, Cunningham C H, Suzuki Y, Willits D A, Willis A F, Yang P C, Tsao P S, McConnell M V, Young M J, et al. A human ferritin iron oxide nano-composite magnetic resonance contrast agent. Magnetic Resonance in Medicine, 2008, 60(5): 1073–1081
110. Jezierska A, Motyl T. Matrix metalloproteinase-2 involvement in breast cancer progression: A mini-review. Medical Science Monitor, 2009, 15(2): RA32–40
111. Ravanti L, Kähäri V. Matrix metalloproteinases in wound repair. International Journal of Molecular Medicine, 2000, 6(4): 391–798
112. Matsumura S, Aoki I, Saga T, Shiba K. A tumor-environment-responsive nanocarrier that evolves its surface properties upon sensing matrix metalloproteinase-2 and initiates agglomeration to enhance t(2) relaxivity for magnetic resonance imaging. Molecular Pharmaceutics, 2011, 8(5): 1970–1974
113. Makino A, Harada H, Okada T, Kimura H, Amano H, Saji H, Hiraoka M, Kimura S. Effective encapsulation of a new cationic gadolinium chelate into apoferritin and its evaluation as an MRI contrast agent. Nanomedicine; Nanotechnology, Biology, and Medicine, 2011, 7(5): 638–646
114. Sanchez P, Valero E, Galvez N, Dominguez-Vera J M, Marinone M, Poletti G, Corti M, Lascialfari A. MRI relaxation properties of water-soluble apoferritin-encapsulated gadolinium oxide-hydroxide nanoparticles. Dalton Transactions (Cambridge, England), 2009, (5): 800–804
115. Lee S, Chen X. Dual-modality probes for *in vivo* molecular imaging. Molecular Imaging, 2009, 8(2): 87–100
116. Cai W, Chen X. Multimodality molecular imaging of tumor angiogenesis. Journal of Nuclear Medicine, 2008, 49(Suppl 2): 113S–128S
117. Cai W, Niu G, Chen X. Multimodality imaging of the HER-kinase axis in cancer. European Journal of Nuclear Medicine and Molecular Imaging, 2008, 35(1): 186–208
118. Wang Z, Huang P, Jacobson O, Wang Z, Liu Y, Lin L, Lin J, Lu N, Zhang H, Tian R, et al. Biomineralization-inspired synthesis of copper sulfide-ferritin nanocages as cancer theranostics. ACS Nano, 2016, 10(3): 3453–3460
119. Xu G, Zhao L, He Z. Performance of whole-body pet/ct for the detection of distant malignancies in various cancers: A systematic review and meta-analysis. Journal of Nuclear Medicine, 2012, 53 (12): 1847–1854
120. Ford E C, Herman J, Yorke E, Wahl R L. 18F-FDG PET/CT for image-guided and intensity-modulated radiotherapy. Journal of Nuclear Medicine, 2009, 50(10): 1655–1665
121. Vach W, Hoilund-Carlsen P F, Gerke O, Weber W A. Generating evidence for clinical benefit of PET/CT in diagnosing cancer patients. Journal of Nuclear Medicine, 2011, 52(Suppl 2): 77S–85S
122. Cai W, Sam Gambhir S, Chen X. Multimodality tumor imaging targeting integrin alphavbeta3. BioTechniques, 2005, 39(6 Suppl): S14–S25
123. Vikram D S, Zweier J L, Kuppusamy P. Methods for noninvasive imaging of tissue hypoxia. Antioxidants & Redox Signaling, 2007, 9(10): 1745–1756
124. Huang P, Lin J, Li W, Rong P, Wang Z, Wang S, Wang X, Sun X, Aronova M, Niu G, et al. Biodegradable gold nanovesicles with an ultrastrong plasmonic coupling effect for photoacoustic imaging and photothermal therapy. Angewandte Chemie International Edition, 2013, 52(52): 13958–13964
125. Yang M, Fan Q, Zhang R, Cheng K, Yan J, Pan D, Ma X, Lu A, Cheng Z. Dragon fruit-like biocage as an iron trapping nanoplatform for high efficiency targeted cancer multimodality imaging. Biomaterials, 2015, 69: 30–37
126. Vannucci L, Falvo E, Failla C M, Carbo M, Fornara M, Canese R, Cecchetti S, Rajsiglova L, Stakheev D, Krizan J, et al. *In vivo* targeting of cutaneous melanoma using an melanoma stimulating hormone-engineered human protein cage with fluorophore and magnetic resonance imaging tracers. Journal of Biomedical Nanotechnology, 2015, 11(1): 81–92
127. Liang M, Fan K, Zhou M, Duan D, Zheng J, Yang D, Feng J, Yan X. H-ferritin-nanocaged doxorubicin nanoparticles specifically target and kill tumors with a single-dose injection. Proceedings of the National Academy of Sciences of the United States of America, 2014, 111(41): 14900–14905

Dr. Xiaoyuan (Shawn) Chen received his PhD in Chemistry from the University of Idaho (1999). After two postdocs at Syracuse University and Washington University in St. Louis, he started his Assistant Professorship in 2002 and then moved to Stanford in 2004. He moved to NIH in 2009 and became a Senior Investigator and Chief of the Laboratory of Molecular Imaging and Nanomedicine (LOMIN) at the National Institute of Biomedical Imaging and Bioengineering (NIBIB), NIH. His current research interests include development of molecular imaging toolbox for better understanding of biology, early diagnosis of disease, monitoring therapy response, and guiding drug discovery/development. His lab puts special emphasis on high-sensitivity nanosensors for biomarker detection and theranostic nanomedicine for imaging, gene and drug delivery, and monitoring of treatment. Dr. Chen has published over 500 peer-reviewed papers (H-index = 101, total citations > 50000 based on Google Scholar) and numerous books and book chapters. He is the founding editor of journal "Theranostics" (2015 IF = 8.854). He received ACS Bioconjugate Chemistry Lecturer Award (2016), NIH Director's Award (2014) and NIBIB Mentor Award (2012). He is also the President of Chinese-American Society of Nanomedicine and Nanobiotechnology (CASNN) and President of the Radiopharmaceutical Science Council (RPSC), Society of Nuclear Medicine and Molecular Imaging (SNMMI).

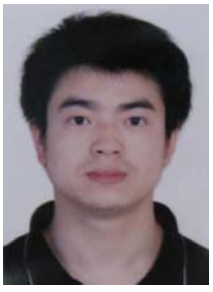

Gang Liu received his MD degree from North Sichuan Medical College (China) in 2002 and PhD degree from Sichuan University (China) in 2009. Subsequently, he focused his training on nanomedicine and molecular imaging at the National Institutes of Biomedical Imaging and Bioengineering (NIBIB), National Institutes of Health (NIH) under the supervision of Dr. Xiaoyuan Chen (2009–2011). In 2012, he joined the Center for Molecular Imaging and Translational Medicine (CMITM), School of Public Health, Xiamen University. Currently he is a Professor of Biomedical and Bioengineering and his research interests include biomaterials, theranostics, and molecular imaging. His scientific work has been published as 100 papers in prestigious journals (Adv. Mater., Nat. Commun., PNAS, etc.), 8 invited book chapters, and 12 patents.